the same. Assuming that the geometrical approach of Nd^{III} to each of the carboxylates is the same, it can be concluded that in the binuclear Nd(DTPA)Nd^{+} complex the second Nd^{III} cation is exchanging between the various carboxylate groups without a distinct preference for one of them.

Conclusions

In summary it is concluded that DTPA coordinates with Ln^{III} cations via the three nitrogens and with the five carboxylate groups (in a monodentate fashion). In all Ln–DTPA complexes one water is present in the first coordination sphere (see Figure 6). The exchange between bound and free DTPA is extremely slow, but exchange broadening occurs in the ^{13}C and ^{1}H NMR spectra as a result of the conformational mobility of the DTPA ligand. The conformational interconversions lead to a pseudomirror plane through the backbone of the middle glycine group. Counterions in the second coordination sphere are probably coordinated to the carboxylate groups and are exchanging almost randomly between them.

This investigation demonstrates that, even in the case of a very asymmetric and mobile complex, a wealth of structural information can be obtained from lanthanide-induced shifts and relaxation rate enhancements. It may be expected that future developments in molecular mechanics will provide us with better geometric models for this type of lanthanide complexes, which will improve the exploitation of the pseudocontact shifts.

Acknowledgment. Thanks are expressed to the Netherlands Foundation for Advancement of Pure Research (ZWO) for financial support, to A. Sinnema for measuring part of the NMR spectra, and to Prof. Dr. A. P. G. Kieboom and Prof. Dr. D. J. Raber for helpful comments.

Contribution from the Department of Chemistry and Biochemistry, University of Windsor, Windsor, Ontario N9B 3P4, Canada

Theory of the Temperature Dependence of the NMR Shift of Intermediate Spin ($S = 1$) Four-Coordinate Ferrous Porphyrins

Bruce R. McGarvey

Received May 24, 1988

The theory of the NMR shift (pseudocontact and contact) for the intermediate spin state ($S = 1$) of four-coordinate ferrous porphyrins is developed for the general case of no axial symmetry. The theory is then fitted to temperature data for the ^{1}H NMR shifts of Fe(OEP) [(2,3,7,8,12,13,17,18-octaethylporphyrinato)iron(II)], Fe(OEC) [(*trans*-7,8-dihydro-2,3,7,8,12,13,17,18-octaethylporphyrinato)iron(II)], and Fe(TPP) [(5,10,15,20-tetraphenylporphyrinato)iron(II)]. It is also fitted to temperature data for the magnetic susceptibility and magnetic anisotropy of solid Fe(TPP) and Fe(PC) [(phthalocyaninato)iron(II)]. The theory assumes the ground state to be a $^{3}A_{2g}$ state that is spin–orbit coupled with the $^{3}E_{g}$ state at energy Δ. In low symmetry the $^{3}E_{g}$ state is split by the energy δ. In solution $\Delta = 600$ cm^{-1} for Fe(OEP) and Fe(OEC) and $\sim$1000 cm^{-1} for Fe(TPP). Δ is reduced to 400 cm^{-1} in solid Fe(TPP) and is -900 cm^{-1} in solid Fe(PC) ($^{3}E_{g}$ ground state). In solution $\delta = -700$ cm^{-1} in Fe(OEC). In Fe(OEP) and Fe(OEC), enough experimental data are available to allow the determination of the geometrical factors for the pseudocontact shift of the methyl resonances from the NMR shifts. The theory is successful in explaining the temperature dependence of the pseudocontact shifts and magnetic susceptibilities but does not fully account for the temperature behavior of the contact shifts.

Introduction

Four-coordinate ferrous porphyrins with an intermediate spin state ($S = 1$) have been studied extensively by using various physical techniques. Assignment of the ground state has proven difficult with three different ground states being proposed as consistent with certain physical properties. The four triplet states considered were $^{3}A_{2g}$ [$(d_{xy})^2(d_{z^2})^2(d_{xz},d_{yz})^2$], $^{3}E_{g}A$ [$(d_{xy})^2(d_{z^2})^1(d_{xz},d_{yz})^3$], $^{3}E_{g}B$ [$(d_{xy})^1(d_{z^2})^2(d_{xz},d_{yz})^3$], and $^{3}B_{2g}$ [$(d_{xy})^1(d_{z^2})^1(d_{xz},d_{yz})^4$]. At various times the states $^{3}A_{2g}$, $^{3}E_{g}A$, and $^{3}B_{2g}$ have been proposed as the ground state.

Most theoretical calculations[1-4] have predicted the $^{3}A_{2g}$ state to be lowest in energy with the $^{3}E_{g}A$ state very close to it. Obara and Kashiwaga[1] have calculated the $^{3}E_{g}A$ state to be only 650 cm^{-1} above the $^{3}A_{2g}$ state in the Fe(II)–porphine complex. They further calculated the $^{3}E_{g}$ state to be 84% $^{3}E_{g}A$ and 12% $^{3}E_{g}B$ due to configurational interaction. They found this mixing was required to explain the quadrupolar results obtained by Mössbauer measurements. Calculations of Dedieu et al.[2] on Fe(TPP) [(5,10,15,20-tetraphenylporphyrinato)iron(II)] show the $^{3}A_{2g}$ state to be below the $^{3}B_{2g}$ state, but their calculations could not give the energy of the $^{3}E_{g}A$ state. Edwards et al.[3] calculated the $^{3}E_{g}A$ state in the Fe(II)–porphine complex to be only 240 cm^{-1} above the $^{3}A_{2g}$ state but proposed, on the basis of their interpretation of Mössbauer and X-ray data in the literature, that the $^{3}E_{g}A$ state was really the ground state. Sontum et al.[4] did an Xα calculation on the Fe(II)–porphine complex that predicts the $^{3}A_{2g}$ state to be 1600 cm^{-1} below the $^{3}E_{g}A$ state. Rawlings et al.[5] are the only ones to calculate $^{3}E_{g}A$ as the ground state, which they found to be about 3800 cm^{-1} below $^{3}A_{2g}$. These calculations, with one exception,[4] do not consider the effect of the spin–orbit interaction, which is about 400 cm^{-1} in magnitude.

The magnetic susceptibility of Fe(PC) [(phthalocyaninato)-iron(II)] was measured by Dale et al.,[6] who fitted the data to an $S = 1$ spin Hamiltonian in which the zero-field interaction was 70 cm^{-1}, $g_{\parallel} = 1.93$, and $g_{\perp} = 2.86$. They claimed the ground state to be $^{3}E_{g}A$, but this may be an error because it contradicts their model, which has a nondegenerate ground state. Barraclough et al.[7] have measured both the magnetic susceptibility and anisotropy

(1) Obara, S.; Kashiwaga, H. *J. Chem. Phys.* **1982**, *77*, 3155.
(2) Dedieu, A.; Rohmer, M. M.; Veillard, A. *Adv. Quantum Chem.* **1982**, *16*, 43.
(3) Edwards, D.; Weiner, B.; Zerner, M. C. *J. Am. Chem. Soc.* **1986**, *108*, 2196.
(4) Sontum, S. F.; Case, D. A.; Karplus, M. J. *J. Chem. Phys.* **1983**, *79*, 2881.
(5) Rawlings, D. C.; Gouterman, M.; Davidson, E. R.; Feller, D. *Int. J. Quantum Chem.* **1985**, *28*, 773.
(6) Dale, B. W.; Williams, R. J. P.; Johnson, C. E.; Thorp, T. L. *J. Chem. Phys.* **1968**, *49*, 3441. Dale, B. W.; Williams, R. J. P.; Edwards, P. R.; Johnson, C. E. *Ibid.* **1968**, *49*, 3445.
(7) Barraclough, C. G.; Martin, R. L.; Mitra, S.; Sherwood, R. C. *J. Chem. Phys.* **1970**, *53*, 1643.

0020-1669/88/1327-4691$01.50/0 © 1988 American Chemical Society

of Fe(PC) and fitted it to the same $S = 1$ spin Hamiltonian with $D = 64$ cm^{-1} and $g_\parallel = g_\perp = 2.74$. They assume the ground state to be $^3B_{2g}$ with no real justification. They point out that D values of this magnitude could only arise when there is an excited state close in energy to the ground state that is coupled to the ground state by the spin–orbit interaction. Boyd et al.[8] have measured the magnetic susceptibility and anisotropy in Fe(TPP) and found that the simple model of a triplet state with a large zero-field splitting did not really fit the measurements. They show that it can be explained by a crystal field model in which the $^3A_{2g}$ state is the ground state with extensive spin–orbit mixing of ^3E_gA and $^3B_{2g}$ states that are close in energy to the $^3A_{2g}$ state.

Quadrupole effects in the Mössbauer spectra of iron(II) porphyrins have been reported by several groups.[9-12] It has proven difficult to explain the results in terms of either the $^3A_{2g}$ or ^3E_g states. Some researchers have claimed the results are most consistent with $^3A_{2g}$[4,10] while others claim ^3E_g[1-3] is more consistent. All claims are accompanied by so many provisos that it appears difficult, if not impossible, to use the quadrupole results to assign the ground state.

Electron density distributions about the iron atom in Fe(PC)[13] at 110 K and in Fe(TPP)[14] at 120 K were determined by X-ray diffraction. In the case of Fe(PC) the results were consistent with that expected for ^3E_gA. For Fe(TPP) the results were less clear, with the electron population of the d orbitals being between that expected for ^3E_gA and $^3A_{2g}$. The population analysis in both cases did not consider the effects of extensive spin–orbit mixing of the two states.

NMR studies of Goff et al.[15] on Fe(TPP) and phenyl-substituted derivatives showed contact shifts that were dominated by π delocalization of spin with little σ delocalization. This would be characteristic of a $^3A_{2g}$ ground state. Mispelter et al.[16] have reported NMR studies on Fe(TPP), Fe(OEP) [(2,3,7,8,12,13,17,18-octaethylporphyrinato)iron(II)], and (α,-α,α,α-*meso*-tetrakis(*o*-pivalamidophenyl)porphyrinato)iron(II), which all show π delocalization in their contact shifts. In further work Mispelter et al.[17] developed a theory for the temperature dependence of the NMR shifts of four-coordinate ($S = 1$) ferrous porphyrins based on a model in which there are two electronic states $^3A_{2g}$ and ^3E_gA close in energy that are strongly intermixed by the spin–orbit coupling. In most systems studied, they found the $^3A_{2g}$ state to be lowest with the ^3E_gA state having energies of 350–1150 cm^{-1}, depending on the ligand. In their model the energy separation of the two states is strongly influenced by any changes in the ligand field along the z axis of the molecule. This was demonstrated in their study of "basket-handle" porphyrins, which showed a strange temperature dependence that could be attributed to very different values of the energy separation of the two states in the different conformers of the complex. Strauss et al.[18] have reported on the temperature dependences of the proton resonances in Fe(OEP) and Fe(OEC) [(*trans*-7,8-dihydro-2,3,7,8,12,13,17,18-octaethylporphyrinato)iron(II)]. They found that although the isotropic shifts in "D_{4h}" Fe(OEP) were linear in T^{-1} with intercepts near zero, the shifts in "C_2" Fe(OEC) could only be fit to straight lines with large nonzero intercepts. Thus the removal of the 4-fold symmetry produced large non-Curie behavior in the NMR shifts. They attributed this to a large temperature-independent paramagnetism, and as will be seen in the theoretical section below, they were essentially correct because only the second-order terms in the van Vleck equation are found to be nonzero in the case of Fe(OEC). Strauss and Pawlik[19] reported similar behavior for the "C_{2v}" complexes Fe(TPC) [(7,8-dihydro-5,10,15,20-tetraphenylporphyrinato)iron(II)] and Fe(TPiBC) [(2,3,7,8-tetrahydro-5,10,15,20-tetraphenylporphyrinato)iron(II)]. Strauss et al.[20] have measured ($\chi_\parallel - \chi_\perp$) for Fe(OEP) and Fe(OEC) by using ^{2}D NMR spectroscopy of *meso*-^{2}D-substituted complexes at different magnetic fields.

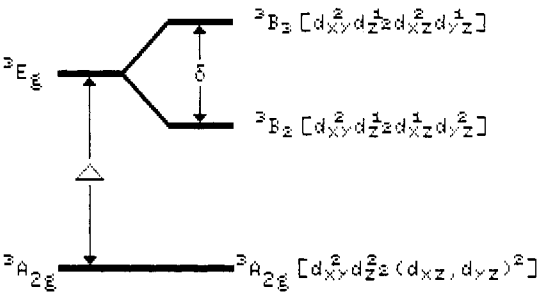

Figure 1. Energy level scheme used in the calculations.

The present work was undertaken to ascertain if the non-Curie temperature dependence observed by Strauss et al.[18,19] could be explained by an extension of the Mispelter et al.[17] theory to the case of lower symmetry. Non-Curie behavior has been observed[21,22] and explained[22,23] in other paramagnetic systems by using the theory of Kurland and McGarvey.[24] In these cases, the complexes had high symmetry and the deviations from Curie behavior were not as pronounced as those observed by Strauss et al.[18,19]

Theory of Pseudocontact Shift

Since Mispelter et al.[17] give no equations for calculating the pseudocontact shift from their model, some details will be given here. According to Kurland and McGarvey[24] the pseudocontact shift can be written as

$$\frac{\Delta H}{H_0} = -\frac{1}{3}\left[\chi_{zz} - \frac{1}{2}(\chi_{xx} + \chi_{yy})\right] F(R,\theta) - \frac{1}{3}[\chi_{xx} - \chi_{yy}]\, G(R,\theta,\phi) \quad (1)$$

$$F(R,\theta) = \frac{3\cos^2\theta - 1}{R^3} \qquad G(R,\theta,\phi) = \frac{\sin^2\theta \cos 2\phi}{R^3}$$

where $\Delta H = (H - H_0)$, χ_{ii} are the principal molecular susceptibilities, R is the distance of the nucleus from the paramagnetic ion, and θ and ϕ are the polar angles for the R vector. χ_{ii} values are calculated from the van Vleck equation[25]

$$\chi_{ii} = \frac{1}{kTq}\{\sum_{\Gamma n,\Gamma m} e^{-\epsilon_\Gamma/kT}\langle \Gamma n|\mu_i|\Gamma m\rangle \times \langle \Gamma m|\mu_i|\Gamma n\rangle + \sum_{\Gamma n,\Gamma' m(\Gamma' \neq \Gamma)} Q_{\Gamma\Gamma'}\langle \Gamma n|\mu_i|\Gamma' m\rangle\langle \Gamma' m|\mu_i|\Gamma n\rangle\} \quad (2)$$

$$\mu_i = -\beta_e(L_i + 2S_i) \quad (3)$$

$$Q_{\Gamma\Gamma'} = \frac{(e^{-\epsilon_\Gamma/kT} - e^{-\epsilon_{\Gamma'}/kT})kT}{\epsilon_{\Gamma'} - \epsilon_\Gamma} \quad (4)$$

$$q = \sum_{\Gamma n} e^{-\epsilon_\Gamma/kT} \quad (5)$$

(8) Boyd, P. D. W.; Buckingham, D. A.; Meeking, R. F.; Mitra, S. *Inorg. Chem.* **1979**, *18*, 3585.
(9) Collman, J. P.; Hoard, J. L.; Kim, N.; Lang, G.; Reed, C. A. *J. Am. Chem. Soc.* **1975**, *97*, 2676.
(10) Lang, G.; Spartalian, K.; Reed, C. A.; Collman, J. P. *J. Chem. Phys.* **1978**, *69*, 5424.
(11) Dolphin, D.; Sams, J. R.; Tsin, T. B.; Wong, K. L. *J. Am. Chem. Soc.* **1976**, *98*, 6970.
(12) Dale, B. W. *Mol. Phys.* **1974**, *28*, 503.
(13) Coppens, P.; Li, L. *J. Chem. Phys.* **1984**, *81*, 1983.
(14) Tanaka, K.; Elkaim, E.; Li, L.; Jue, Z. N.; Coppens, P.; Landrum, J. *J. Chem. Phys.* **1986**, *84*, 6969.
(15) Goff, H.; La Mar, G. N.; Reed, C. A. *J. Am. Chem. Soc.* **1977**, *99*, 3641.
(16) Mispelter, J.; Momenteau, M.; Lhoste, J. M. *Mol. Phys.* **1977**, *33*, 1715.
(17) Mispelter, J.; Momenteau, M.; Lhoste, J. M. *J. Chem. Phys.* **1980**, *72*, 1003.
(18) Strauss, S. H.; Silver, M. E.; Long, K. M.; Thompson, R. G.; Hudgens, R. A.; Spartalian, K.; Ibers, J. A. *J. Am. Chem. Soc.* **1985**, *107*, 4207.
(19) Strauss, S. H.; Pawlik, M. J. *Inorg. Chem.* **1986**, *25*, 1921.
(20) Strauss, S. H.; Long, K. M.; Magerstädt, M.; Gansow, O. *Inorg. Chem.* **1987**, *26*, 1185.
(21) Jesson, J. P.; La Mar, G. N.; Meakin, P. *J. Am. Chem. Soc.* **1971**, *93*, 1286.
(22) Gamp, E.; Shinamoto, R.; Edelstein, N.; McGarvey, B. R. *Inorg. Chem.* **1987**, *26*, 2177.
(23) McGarvey, B. R. *J. Chem. Phys.* **1970**, *53*, 86.
(24) Kurland, R. J.; McGarvey, B. R. *J. Magn. Reson.* **1970**, *2*, 286.

where Γ and Γ' are indices that label energy levels in the absence of a magnetic field and n and m label particular degenerate states within a given energy level ϵ_Γ, β_e is the Bohr magneton, L the total angular momentum operator, and S the total spin operator.

We define Δ as the energy separation between the mean energy of the ^3E_gA states and the $^3A_{2g}$ state before the application of the spin–orbit interaction. When the ligand field has a symmetry less than 4-fold or 3-fold about the axis perpendicular to the plane (z axis) of the molecule, the ^3E_gA state splits into $^3B_2$ [$(d_{xy})^2(d_{z^2})^1(d_{xz})^1(d_{yz})^2$] and $^3B_3$ [$(d_{xy})^2(d_{z^2})^1(d_{xz})^2(d_{yz})^1$] states. We define δ as the energy difference between $^3B_2$ and $^3B_3$ states (see Figure 1) in the absence of a spin–orbit interaction. It should be noted that Mispelter et al.[17] appear to define Δ as done here in their Figure 9 but their Figure 10 and quoted values of Δ in the text show that their equations have *defined their* Δ *as the negative of that used here.*

It is convenient in the calculation to use the "hole" formulation for the wave functions in which the spin–orbit operator becomes

$$H_{LS} = -\lambda\sum_n (l\cdot s)_n \tag{6}$$

where λ is the individual electron spin–orbit parameter. The wave functions for the nine states involved are

$$A_{2g}(\pm) = (1/\sqrt{2})[d_{xz}^{+}d_{yz}^{+} \pm d_{xz}^{-}d_{yz}^{-}]$$

$$A_{2g}(0) = (1/\sqrt{2})[d_{xz}^{+}d_{yz}^{-} + d_{xz}^{-}d_{yz}^{+}]$$

$$B_2A(\pm) = (1/\sqrt{2})[d_{z^2}^{+}d_{xz}^{+} \pm d_{z^2}^{-}d_{xz}^{-}]$$

$$B_2A(0) = (1/\sqrt{2})[d_{z^2}^{+}d_{xz}^{-} + d_{z^2}^{-}d_{xz}^{+}]$$

$$B_3A(\pm) = (i/\sqrt{2})[d_{z^2}^{+}d_{yz}^{+} \pm d_{z^2}^{-}d_{yz}^{-}]$$

$$B_3A(0) = (i/\sqrt{2})[d_{z^2}^{+}d_{yz}^{-} + d_{z^2}^{-}d_{yz}^{+}] \tag{7}$$

The $i = \sqrt{-1}$ in B_3 functions is required to obtain real matrices in the spin–orbit calculation. Obara and Kashiwaga[1] have suggested that configuration interaction mixes E_gA and E_gB states, and we have found it necessary to include this to explain the experimental results. Thus the ^3E_g functions are rewritten

$$B_2(\pm) = M_1B_2A(\pm) + N_1B_2B(\pm)$$

$$B_2(0) = M_1B_2A(0) + N_1B_2B(0)$$

$$B_3(\pm) = M_2B_3A(\pm) + N_2B_3B(\pm)$$

$$B_3(0) = M_2B_3A(0) + N_2B_3B(0) \tag{8}$$

where

$$B_2B(\pm) = (1/\sqrt{2})[d_{xy}^{+}d_{yz}^{+} \pm d_{xy}^{-}d_{yz}^{-}]$$

$$B_2B(0) = (1/\sqrt{2})[d_{xy}^{+}d_{yz}^{-} + d_{xy}^{-}d_{yz}^{+}]$$

$$B_3B(\pm) = (i/\sqrt{2})[d_{xy}^{+}d_{xz}^{+} \pm d_{xy}^{-}d_{xz}^{-}]$$

$$B_3B(0) = (i/\sqrt{2})[d_{xy}^{+}d_{xz}^{-} + d_{xy}^{-}d_{xz}^{+}] \tag{9}$$

The $^3B_{2g}$ state ($d_{xy}d_{z^2}$) has not been included because all theoretical calculations[1-5] put it at a much higher energy so that it would contribute little to the calculation. Also excited quintet states have been excluded from consideration.

Application of the spin–orbit operator H_{LS} to the nine functions in eq 7–9 gives rise to four determinants:

	$A_{2g}(+)$	$B_2(0)$	
$A_{2g}(+)$	$-\epsilon$	$-\lambda_1/2$	$= 0$
$B_2(0)$	$-\lambda_1/2$	$\Delta - \delta/2 - \epsilon$	

(10)

	$A_{2g}(-)$	$B_3(0)$	
$A_{2g}(-)$	$-\epsilon$	$-\lambda_2/2$	$= 0$
$B_3(0)$	$-\lambda_2/2$	$\Delta + \delta/2 - \epsilon$	

(11)

	$B_2(-)$	$B_3(+)$	
$B_2(-)$	$\Delta - \delta/2 - \epsilon$	$-\lambda_0/2$	$= 0$
$B_3(+)$	$-\lambda_0/2$	$\Delta + \delta/2 - \epsilon$	

(12)

	$A_{2g}(0)$	$B_2(+)$	$B_3(-)$	
$A_{2g}(0)$	$-\epsilon$	$-\lambda_1/2$	$\lambda_2/2$	
$B_2(+)$	$-\lambda_1/2$	$\Delta - \delta/2 - \epsilon$	$-\lambda_0/2$	$= 0$
$B_3(-)$	$\lambda_2/2$	$-\lambda_0/2$	$\Delta + \delta/2 - \epsilon$	

(13)

where

$$\lambda_0 = \lambda(M_2M_1 - N_2N_1)$$

$$\lambda_1 = \lambda(\sqrt{3}M_1 + N_1)$$

$$\lambda_2 = \lambda(\sqrt{3}M_2 + N_2) \tag{14}$$

From these determinants we can calculate the nine energy states and their wave functions. These functions take the form

$$\psi_{1,3} = a_{1,3}A_{2g}(+) + b_{1,3}B_2(0)$$

$$\psi_{2,4} = c_{2,4}A_{2g}(-) + d_{2,4}B_3(0) \tag{15}$$

$$\psi_{6,8} = i_{6,8}B_2(-) + h_{6,8}B_3(+)$$

$$\psi_{5,7,9} = e_{5,7,9}A_{2g}(0) + f_{5,7,9}B_2(+) + g_{5,7,9}B_3(-)$$

where the lower index is assigned the lower energy.

In calculating χ_{ii}, we will follow the general practice of introducing an orbital reduction factor κ to account for covalency affects. This is done by rewriting eq 3 as

$$\mu_i = -\beta_e(\kappa L_i + 2S_i) \tag{16}$$

Applying eq 2, 4, 5, 15, and 16, we obtain for the molecular susceptibilities the following equations:

$$\chi_{xx} = \left(\frac{2\beta_e^2}{kTq}\right)\{\sum_{i=1,3}\sum_{j=5,7,9}[2(a_ie_j + b_if_j) + \kappa(\sqrt{3}M_1 + N_1) \times (b_ie_j + a_if_j)]^2Q_{ij} + \sum_{i=2,4}\sum_{j=6,8}[2d_ih_j + \kappa(\sqrt{3}M_1 + N_1)c_ii_j]^2Q_{ij}\} \tag{17}$$

$$\chi_{yy} = \left(\frac{2\beta_e^2}{kTq}\right)\{\sum_{i=2,4}\sum_{j=5,7,9}[2(c_ie_j - d_ig_j) + \kappa(\sqrt{3}M_2 + N_2) \times (d_ie_j - c_ig_j)]^2Q_{ij} + \sum_{i=1,3}\sum_{j=6,8}[2b_ii_j + \kappa(\sqrt{3}M_2 + N_2)a_ih_j]^2Q_{ij}\} \tag{18}$$

$$\chi_{zz} = \left(\frac{2\beta_e^2}{kTq}\right)\{\sum_{i=6,8}\sum_{j=5,7,9}[2(h_ig_j + i_if_j) + \kappa(M_2M_1 - N_2N_1) \times (h_if_j + i_ig_i)]^2Q_{ij} + \sum_{i=1,3}\sum_{j=2,4}[2a_ic_j + \kappa(M_2M_1 - N_2N_1)b_id_j]^2Q_{ij}\} \tag{19}$$

Theory of Contact Shift

The more general form of the equation[24] to calculate paramagnetic shifts is obtained from eq 3 by replacing one of the two μ_i operators by the operator $A_{Ni}/g_N\beta_N$:

(25) Van Vleck, J. H. *Theory of Electric and Magnetic Susceptibilities*; Oxford University Press: London/New York, 1933.

$$A_{Ni}/g_N\beta_N = \left(\frac{8\pi}{3}\right)g_e\beta_e\sum_j \delta(r_j)(s_i)_j + g_e\beta_e\sum_j [3(\vec{s}_j\cdot\vec{r}_j)(r_i)_j - r_j^2(s_i)_j]r_j^{-5} + 2\beta_e\sum_j r_j^{-3}(l_i)_j \quad (20)$$

If we assume that the main delocalization of spin onto the ligand is into the π aromatic system, then the first term in eq 20 can be represented by

$$A_{Ni}/g_N\beta_N = \rho_\pi\left(\frac{Q}{g_N\beta_N}\right)S_i \quad (21)$$

where ρ_π is the spin density at the carbon atom in the π system closest to the proton in question and Q is the parameter in the McConnell equation[26] relating ρ_π with the hyperfine constant observed in ESR. In most previous calculations of the "contact shifts", eq 21 is all that was considered. It has not been recognized that the second term in eq 20 can give rise to a comparable term for protons directly attached to the aromatic carbon atom. If we assume that the C(π)–H bond lies in the xy plane and makes an angle α with the principal x axis, then inclusion of the second dipolar term gives

$$A_{Nx}/g_N\beta_N = \rho_\pi\left[\frac{Q}{g_N\beta_N} + \frac{g_e\beta_e}{R^3}(3\cos^2\alpha - 1)\right]S_x$$

$$A_{Ny}/g_N\beta_N = \rho_\pi\left[\frac{Q}{g_N\beta_N} + \frac{g_e\beta_e}{R^3}(3\sin^2\alpha - 1)\right]S_y$$

$$A_{Nz}/g_N\beta_N = \rho_\pi\left[\frac{Q}{g_N\beta_N} - \frac{g_e\beta_e}{R^3}\right]S_z \quad (22)$$

For protons attached to an aromatic carbon atom, $(g_e\beta_e/R^3)$ is about the same magnitude as $(Q/g_N\beta_N)$ and of opposite sign. If $\langle S_x\rangle = \langle S_y\rangle = \langle S_z\rangle$, then the dipolar term would average to zero, but in the systems studied here this will not be the case.

Mispelter et al.[17] used essentially eq 21 when they calculated the contact shift. They also assumed $Q\rho_\pi$ to be the same for both $^3A_{2g}$ and ^3E_gA functions, which does not seem reasonable since in $^3A_{2g}$ both unpaired spins are in d_{xz},d_{yz} orbitals that interact with the π system while in ^3E_gA only one electron is found in a d_{xz},d_{yz} orbital with the other one in a d_{z^2} orbital. Sontum et al.[4] have calculated the value of ρ_π at the meso and β-pyrrole carbons for both the $^3A_{2g}$ and ^3E_gA states and find the ^3E_gA state has a positive spin density about half of that of the $^3A_{2g}$ state at the pyrrole atom. For the meso carbon, ρ_π is negative and about the same for both states. In calculating the π contribution to the shift, we have assumed ρ_π in the E_g functions to be half that in the A_{2g} functions. In practice this has made little difference in the systems we have analyzed because they have a $^3A_{2g}$ ground state that dominates the final calculated shifts.

The contact shift equations are obtained from eq 17–19 by first dividing by $(-2\beta_e)$ and then setting $\kappa = 0$ for one of the two parts of the squared terms and in the same term dividing those product coefficients involving ^3E_g functions (b, d, f, g, i, h) by 2, and finally multiplying by the appropriate coefficient of S_i in eq 22.

Application of Theory to Experimental Systems

The theory will first be applied to the Fe(OEP) and Fe(OEC) molecules because we have more experimental data for them that will be needed in the analysis. Also, as will be seen later, there are certain features in these molecules that make the analysis easier to do. The results are found to be rather insensitive to the exact value chosen for the spin–orbit parameter, λ. A change in λ of a few tens of reciprocal centimeters just requires a change of a few tens of reciprocal centimeters in the value of Δ to get the same result. We have chosen to keep $\lambda = 412$ cm^{-1}, which is the value used by Mispelter et al.[17]

A. Fe(OEP). Strauss et al.[20] have measured $(\chi_\parallel - \chi_\perp)$ to be -7.9×10^{-3} cm^3/mol at 298 K for Fe(OEP) from ^{2}D NMR

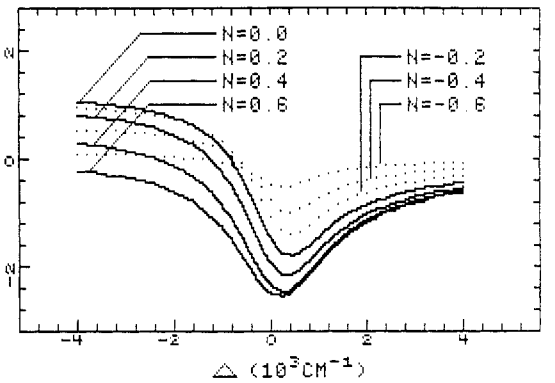

Figure 2. Plot of $(\chi_\parallel - \chi_\perp)$ at 300 K vs Δ for different values of N, $\delta = 0$ and $\kappa = 1.0$. The units for χ are $(\beta_e^2/k) \times 10^{-2}$. o

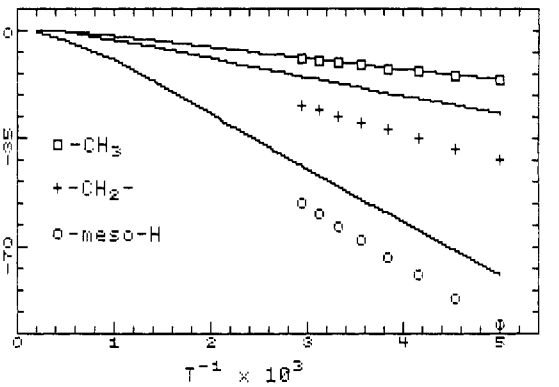

Figure 3. Plot of ^{1}H NMR shifts of Fe(OEP) vs T^{-1}. The solid lines are calculated pseudocontact shifts. Shifts are in ppm.

spectral data for the *meso*-^{2}D-substituted complex. In Figure 2 is plotted the calculated values for $(\chi_\parallel - \chi_\perp)$ at 300 K versus Δ for $\delta = 0$, $\kappa = 1.0$ and various values of $N = N_1 = N_2$. The marked dependence of $(\chi_\parallel - \chi_\perp)$ upon N is quite evident in Figure 2. The values of χ are given in units of $(\beta_e^2/k) \times 10^{-2}$ for convenience. The experimental value of $(\chi_\parallel - \chi_\perp)$ is -2.1 in these units. It can be seen that this value is only reached for $N \gtrsim 0.2$. For $\kappa = 0.9$, N must be greater than 0.3, and for $\kappa = 0.8$, the calculated value is below the experimental value for all reasonable values of N. Since $\kappa = 0.9$ has produced better fits for Fe(OEC) than $\kappa = 1.0$, we have taken $\kappa = 0.9$ for all calculations in this work. For $N = 0.4$ and $\kappa = 0.9$, the values of Δ that give the experimental value of $(\chi_\parallel - \chi_\perp)$ are 0 and 600 cm^{-1}. We chose $\Delta = 600$ cm^{-1} because plots of $(\chi_\parallel - \chi_\perp)$ vs T^{-1} for $\Delta < 500$ cm^{-1} show a pronounced non-Curie temperature behavior, which when fitted to a straight line between 200 and 320 K will give a nonzero intercept much greater than that found for the $-CH_3$ resonance, which is expected to be entirely pseudocontact in origin.

Having now estimated Δ, N, and κ, we can fit the $-CH_3$ resonance in Fe(OEP) to theory and determine the geometrical factor $F(R,\theta)$. The value obtained was -2.57×10^{21} cm^{-3}, which compares well with the average value of -2.87×10^{21} cm^{-3} calculated from the crystal structure.[18] Since the CH_3 group is somewhat free to flop around, we have estimated the geometrical factor for the group when it is as far above or below the plane of the porphyrin ring as possible. This value is -2.54×10^{21} cm^{-3}, which is very close to the value determined here.

In Figure 3 are plotted the calculated pseudocontact shifts for all three resonances of Fe(OEP). The value of $F(R,\theta)$ for the $-CH_2-$ group is -4.57×10^{21} cm^{-3} from the crystal structure and -4.26×10^{21} cm^{-3} for CH_3 above the molecular plane. We have used the second value in Figure 3. The value for meso-H was -12.19×10^{21} cm^{-3} as determined from the crystal structure. For both the $-CH_2-$ and meso-H resonances, the experimental shifts are further downfield than the pseudocontact shifts indicating a contact shift of the same sign for both.

In the fit of the contact part of the shift to the theory, $Q = -63.1$ MHz was used for the meso-H and $Q = 57.2$ MHz for the $-CH_2-$

(26) McConnell, H. M. *J. Chem. Phys.* **1956**, *24*, 764; *Proc. Natl. Acad. Sci. U.S.A.* **1957**, *43*, 721.

Table I. Parameters Used To Calculate the Fitted NMR Shifts

resonance	$F(R,\theta)$, $cm^{-3} \times 10^{-21}$	$G(R,\theta,\phi)$, $cm^{-3} \times 10^{-21}$	Q, MHz	$g_e\beta_e g_N\beta_N/R^3$, MHz	ρ_π
Fe(OEP): Δ = 600 cm^{-1}; δ = 0; λ = 412 cm^{-1}; $N_1 = N_2$ = 0.4; κ = 0.9					
$-CH_3$	−2.57[a]				
$-CH_2-$	−4.26[b]		57.2	9.5	0.0021
meso-H	−12.19[b]		−63.1	79.1	−0.0033
Fe(OEC): Δ = 600 cm^{-1}; δ = −700 cm^{-1}; λ = 412 cm^{-1}; $N_1 = N_2$ = 0.4; κ = 0.9					
$-CH_3$(e)	−2.19[a]	−2.62[b]			
$-CH_3$(h)	−2.19[a]	+2.62[b]			
$-CH_3$(i)	−0.53[a]	+2.86[a]			
$-CH_2-$(c)	−4.26[b]	−3.57[b]	57.2	9.5	0.0037
$-CH_2-$(d)	−4.26[b]	−3.57[b]	57.2	9.5	0.0058
$-CH_2-$(g)	−4.26[b]	+3.57[b]	57.2	9.5	0.0002
β-H	−6.88[b]	+6.31[b]	57.2	9.5	0.0051
meso-H(a)	−11.79[b]	0.0	−63.1	79.1	−0.0022
meso-H(b)	−11.79[b]	0.0	−63.1	79.1	−0.0012
$-CH_AH_B$(1)	−5.28[b]	+4.80[b]			
$-CH_AH_B$(2)	−6.48[b]	+4.63[b]			
$-CH_AH_B$(3)	−4.10[b]	+3.66[b]			
Fe(TPP): Δ = 1075 cm^{-1}; δ = 0; λ = 412 cm^{-1}; $N_1 = N_2$ = 0.4; κ = 0.9					
meta H	−1.67[b]				
ortho H	−3.61[b]				
pyrrole H	−7.03[b]		−63.1	79.1	0.0075

[a] Calculated from experimental shift. [b] Calculated from molecular structure.

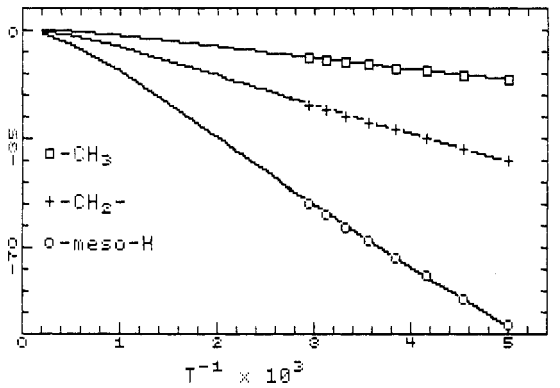

Figure 4. Plot of ^1H NMR shifts of Fe(OEP) vs T^{-1}. The solid lines are total calculated shifts. Shifts are in ppm.

group. These are values taken from ESR studies of benzene type radicals. The Q used for $-CH_2-$ groups was determined for $-CH_3$ groups attached to benzene rings. The value of $(g_e\beta_e g_N\beta_N/R^3)$ used for the meso-H was 79.1 MHz, which corresponds to a C–H distance of 1.0 Å. The corresponding value for the $-CH_2-$ group was estimated to be about 9.5 MHz. The fitted values of ρ_π are given in Table I along with the other parameters, and the total calculated shift vs T^{-1} is shown in Figure 4. For the meso-H resonance, the effect of ignoring the dipolar term and assuming only a contact shift is a 30% change in ρ_π to −0.0023 and a somewhat poorer fit to the experimental shifts. Assuming the hyperfine interactions to be identical for both the $^3A_{2g}$ and ^3E_g states, as Mispelter et al.[17] did, changes ρ_π by only 6% to −0.0031. In the case of the $-CH_2-$ resonance, the dipolar term has less than a 5% effect on the value of ρ_π.

B. Fe(OEC). The value of $[\chi_{zz} - {}^1/_2(\chi_{xx} + \chi_{yy})]$ for Fe(OEC) has also been determined by Strauss et al.[20] to be -7.6×10^{-3} cm^3/mol at 298 K, which is nearly the same as that found for Fe(OEP). In Figure 5 is plotted $[\chi_{zz} - {}^1/_2(\chi_{xx} + \chi_{yy})]$ at 300 K vs Δ for several values of δ when N = 0.4 and κ = 1.0. In the region of $\Delta > 0$, δ has no appreciable effect on the value of $[\chi_{zz} - {}^1/_2(\chi_{xx} + \chi_{yy})]$. This is because δ has little effect on χ_{zz} and nearly equal but opposite effects on χ_{xx} and χ_{yy}. Thus we can assume the same values of Δ = 600 cm^{-1}, N = 0.4, and κ = 0.9 that were found for Fe(OEP), and our only problem is to find a way to estimate δ. This can be done by examining the $-CH_3$ resonances designated as e and h by Strauss et al.[18] If we take the principal x axis to be the N_3–Fe–N_2 direction in their Figures

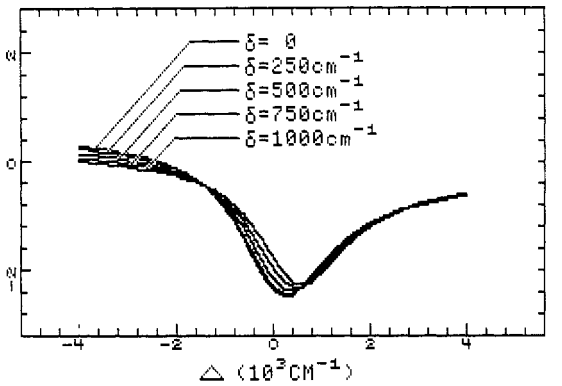

Figure 5. Plot of $[\chi_{zz} - {}^1/_2(\chi_{xx} + \chi_{yy})]$ at 300 K vs Δ for different values of δ. N = 0.4 and κ = 1.0. The units for χ are $(\beta_e^2/k) \times 10^{-2}$.

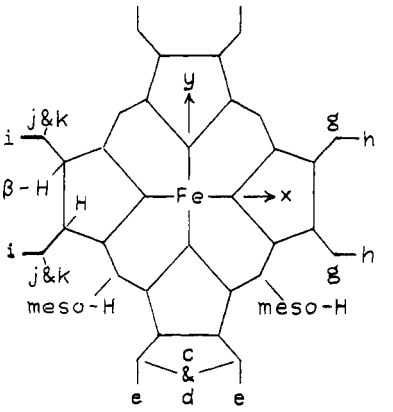

Figure 6. Fe(OEC) molecule with location of the various protons discussed in the paper. The coordinate axes used in the analysis are also shown. The x axis is the C_2 symmetry axis.

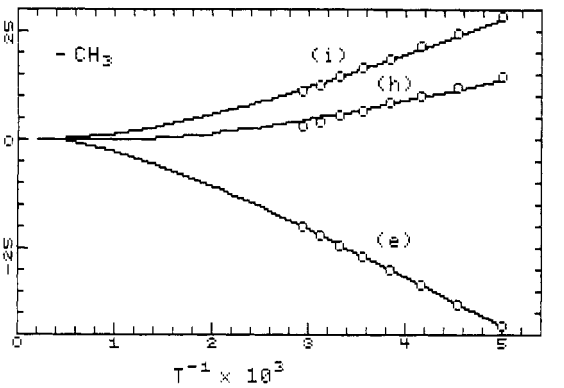

Figure 7. Plot of $-CH_3$ NMR shifts of Fe(OEC) vs T^{-1}. Solid lines are calculated pseudocontact shifts. Shifts are in ppm.

1 and 2, which bisects the more saturated pyrroline ring, then by intensity we can identify the e resonances as those methyls close to the y axis and the h resonances as those close to the x axis. The i resonance belongs to the CH_3 in the ethyl groups attached to the pyrroline ring. The location of these groups and all others identified by Strauss et al.[18] in the molecule are shown in Figure 6. If we now assume that the $F(R,\theta)$ geometrical factor is essentially the same for both the e and h resonances, then the differences between the two resonances depends only on the $(\chi_{xx} - \chi_{yy})$ term in eq 1. This term is found to be very sensitive to the value of δ. The geometrical factor $G(R,\theta,\phi)$ is $\pm 2.62 \times 10^{21}$ cm^{-3} for the h and e resonances as calculated from the crystal structure.[18] This term is much less sensitive to the orientation of the CH_3 group than the $F(R,\theta)$ term because the θ and ϕ parts change in opposite directions. It was found that the difference between the e and h resonances could be fitted to $\delta = -700$ cm^{-1} if $G(R,\theta,\phi) = \pm 2.62 \times 10^{21}$ cm^{-3}.

The total shift for e and h resonances can now be fitted by using $F(R,\theta) = -2.19 \times 10^{21}$ cm^{-3}. This is somewhat smaller than that

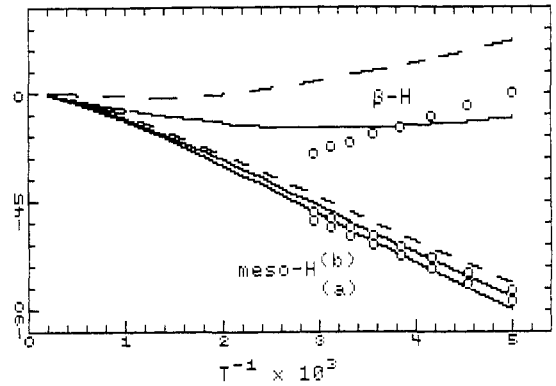

Figure 8. Plot of β-H and meso-H NMR shifts of Fe(OEC) vs T^{-1}. Dahsed lines are calculated pseudocontact shifts, and solid lines are total calculated shifts. Shifts are in ppm.

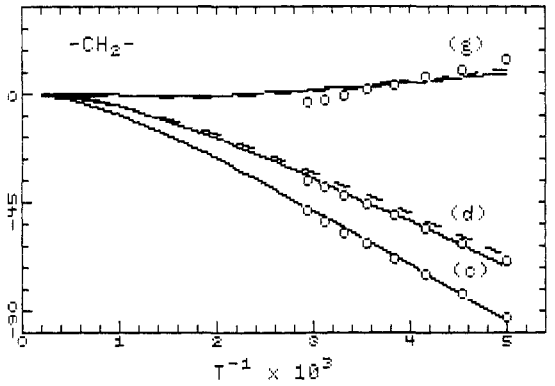

Figure 9. Plot of $-CH_2-$ NMR shifts of Fe(OEC) vs T^{-1}. Dashed lines are calculated pseudocontact shifts, and solid lines are total calculated shifts. Shifts are in ppm.

found for Fe(OEP) but is reasonable considering the puckered nature of the macrocycle in Fe(OEC) vs the planar conformation of Fe(OEP). The calculated and experimental shifts for all CH_3 groups are plotted in Figure 7. For resonance i the value of $G(R,\theta,\phi)$ was estimated from the ratio of experimental intercepts for the fitted straight lines of resonances i and h, as it has been found in the calculations that this intercept is primarily determined by the $(\chi_{xx} - \chi_{yy})$ term in the pseudocontact shift. All fitted values are given in Table I.

The calculated pseudocontact shifts for meso-H and β-H resonances are shown as dashed lines in Figure 8, and for those $-CH_2-$ groups are shown in Figure 9. The geometrical factors as calculated from the crystal structure[18] are given in Table I. The solid lines in Figure 8 and 9 are the fitted curves including the contact shift. The parameters used in fitting are given in Table I.

The symmetry-related $-CH_2-$ groups attached to the pyrroline ring give two resonances and are particularly difficult to analyze. It would be of some interest to calculate the pseudocontact shift to determine if there is any contact shift. The geometrical factors have been calculated for the three staggered conformations of the CH_2 group by using crystal structure data, and the pseudocontact shifts for these three orientations are shown as solid lines in Figure 10 along with the experimental shifts. These conformations assumed the ring had the same conformation as in the crystal, which places the CH_2 near the plane of the molecule. The rather small value found for $F(R,\theta)$ for CH_3(i) suggests that in solution the ring may be in the other conformation, which brings the ethyl group further above the plane of the molecule, making $F(R,\theta)$ much smaller for both the CH_2 and CH_3 groups. In Figure 10 the solid line is the pseudocontact shift calculated for $F(R,\theta) = -2 \times 10^{21}$ cm^{-3} and $G(R,\theta,\phi) = 4.7 \times 10^{21}$ cm^{-3}. It is apparent that the existence of a contact shift at this site is not certain as the bulk of the shift could be pseudocontact.

C. Fe(TPP). In this case we have no solution measurement of $(\chi_\parallel - \chi_\perp)$, obtained independently of the paramagnetic shift,

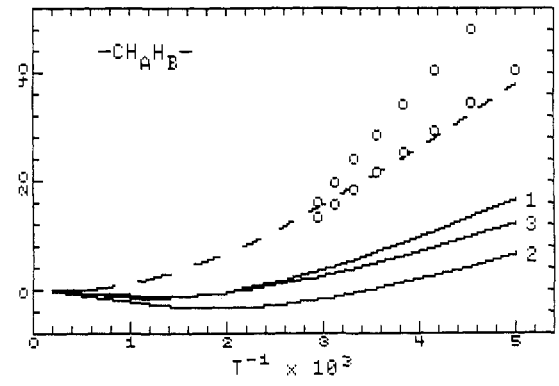

Figure 10. Plot of $-CH_AH_B-$ NMR shifts of Fe(OEC) vs T^{-1}. Solid lines are calculated pseudocontact shifts for three staggered conformations of the CH_2 group. The dashed line is a pseudocontact shift calculated for different geometrical factors as explained in the text. Shifts are in ppm.

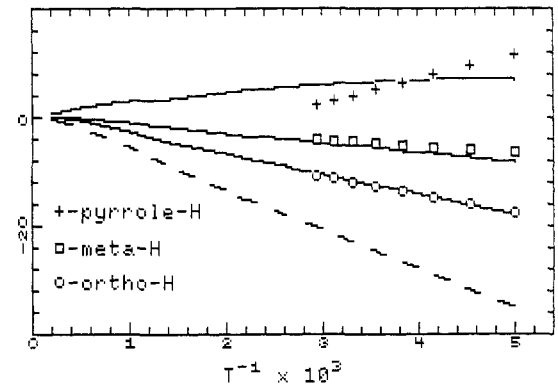

Figure 11. Plot of ^{1}H NMR shifts in Fe(TPP) vs T^{-1}. The dashed line is a calculated pseudocontact shift for pyrrole H, and solid lines are total calculated shifts. Shifts are in ppm.

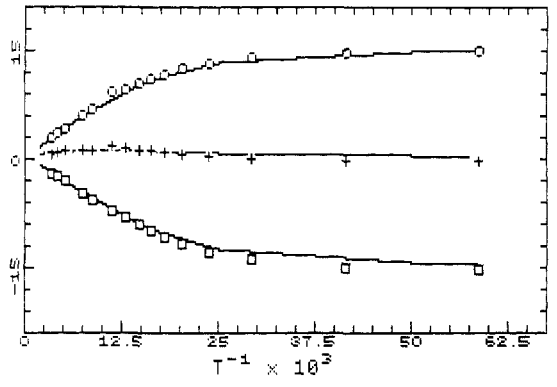

Figure 12. Plot of $\chi_\perp$ (O), $\chi_\parallel$ (+), and $(\chi_\parallel - \chi_\perp)$ (□) for Fe(TPP) solid vs T^{-1}. Solid lines are calculated values. The units for χ are $(\beta_e^2/k) \times 10^{-2}$.

so we must use the pseudocontact shift of the phenyl hydrogens to estimate Δ. Using the shifts reported by Strauss and Pawlik[19] and the geometric factors calculated by Goff et al.,[15] we find a Δ of 1075 cm^{-1} from fitting the ortho-H shifts and 1400 cm^{-1} from fitting the meta-H shifts when $\lambda = 412$ cm^{-1}, $N = 0.4$, and $\kappa = 0.9$. Δ = 900 and 1250 cm^{-1} if $N = 0.2$ is assumed instead of 0.4. Mispelter et al.[16] have reported evidence of a contact shift at the ortho site from ^{19}F NMR spectra of fluoro-substituted Fe(TPP). They also report different values for the geometric factors. The best we can probably say is that Δ is somewhere between 900 and 1300 cm^{-1}. In Figure 11 is plotted the calculated shifts for Δ = 1075 cm^{-1} and $N = 0.4$. The solid lines are the total shift, and the dashed line is just the pseudocontact shift for the pyrrole hydrogen. For the pyrrole hydrogen $\rho_\pi = 0.0075$ was used in the calculation.

The anisotropy of the magnetic susceptibility has been measured in solid Fe(TPP) by Boyd et al.[8] The theory developed in this

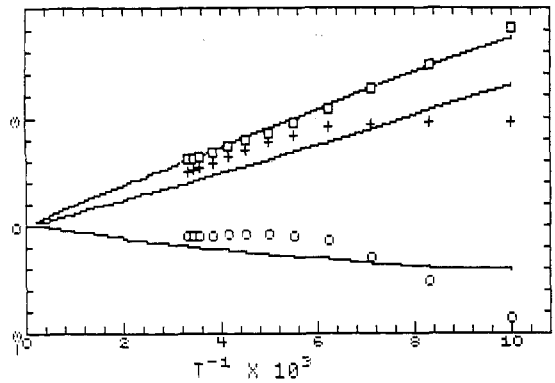

Figure 13. Plot of $\chi_\perp$ (○), $\chi_\parallel$ (+), and $(\chi_\parallel - \chi_\perp)$ (□) for Fe(PC) solid vs T^{-1}. Solid lines are calculated values. The units for χ are $(\beta_e^2/k) \times 10^{-2}$.

paper has been fitted to data extracted from their figures, and the results are plotted in Figure 12. For convenience the susceptibility is plotted in units of $(\beta_e^2/k) \times 10^{-2}$. The best fit was obtained with $\lambda = 412$ cm^{-1}, $\Delta = 400$ cm^{-1}, $N = 0.2$, and $\kappa = 0.9$. Somewhat poorer fits were obtained with $N = 0.3$ and $\Delta = 250$ cm^{-1} and with $N = 0.1$ and $\Delta = 500$ cm^{-1}. The lower temperature values were quite sensitive to the choice of N. It appears that the value of Δ and hence the values of $(\chi_\parallel - \chi_\perp)$ are much different in the solid from those found for the molecule in a noncoordinating solvent.

D. Fe(PC). There are no NMR data to fit, but the magnetic anisotropy has been measured in the solid by Barraclough et al.[7] These data have been fitted to the theory by first fitting $\chi_\perp$. Good fits were obtained for $\Delta = 1900$ cm^{-1} and $N = 0.3$, and $\Delta = -900$ cm^{-1} and $N = 0.3$. However, $\Delta = 1900$ cm^{-1} gave very poor fits for $\chi_\parallel$ and $(\chi_\parallel - \chi_\perp)$, $\Delta = -900$ cm^{-1} gave values of $\chi_\parallel$ and $(\chi_\parallel - \chi_\perp)$ of the correct magnitude, but the fit is less than satisfying. The results are plotted in Figure 13.

E. Fe(TPC). Too little data are available to analyze the data of Strauss and Pawlik[19] in the manner used for Fe(OEC). One of the main drawbacks is that the phenyl groups that supply the only shifts governed just by the pseudocontact shift are located at the meso position of the ring where there is no contribution from the $(\chi_{xx} - \chi_{yy})$ term of the pseudocontact shift. This makes it difficult to estimate the parameter δ. Also there is a lack of good crystal data. Attempts to do something with the data show that Δ is probably between 1000 and 3000 cm^{-1}.

Discussion

The results show that the theory developed here is quite adequate to explain the pseudocontact shift in these complexes if we assume some configuration interaction between the ^3E_gA and ^3E_gB states. The large non-Curie-like temperature dependences observed for complexes that lack axial symmetry have been explained in terms of the non-Curie behavior of the pseudocontact shift. Small energy differences in the two states arising from the E_g state are found sufficient to produce large deviations from Curie behavior.

The theory has many parameters but only Δ, δ, and the relative magnitude of the $G(R,\theta,\phi)$ structural parameter to the $F(R,\theta)$ structural parameter have any major effect on the shape of the shift vs T^{-1} curve. For the temperature range in which solution NMR shifts can be measured, it is always possible to fit the shift to a linear equation with the T^{-1} variable. The non-Curie behavior is detected in this case by the presence of a sizable nonzero intercept. For compounds with a small distortion from axial symmetry ($\delta \approx 0$), deivations from Curie behavior become noticeable only for Δ in the range +500 to −1000 cm^{-1}, and the deviations are never as pronounced as those seen in Fe(OEC). This is because the Q_{ij} terms involving the ground state approach unity as T^{-1} approaches zero. Thus each χ_{ii} term has a T^{-1} dependence in the high-temperature region, and therefore $(\chi_\parallel - \chi_\perp)$ has a T^{-1} dependence also. The situation is different for the $(\chi_{xx} - \chi_{yy})$ term, which has a zero slope in a T^{-1} plot for high temperatures. Thus non-Curie behavior is most pronounced when there is a large contribution from the $(\chi_{xx} - \chi_{yy})$ term in the pseudocontact shift, and this occurs when δ is not zero and $G(R,\theta,\phi)$ has a magnitude comparable with that of $F(R,\theta)$. Values of a few hundred reciprocal centimeters for δ are sufficient to produce large values for $(\chi_{xx} - \chi_{yy})$. Deviations from Curie behavior seem to be less pronounced in the contact shift equation and come mostly from the dipolar term, and this in turn is important only for meso- and pyrrole hydrogens.

The value of Δ depends on the energy of the d_{z^2} orbital relative to the d_{xz}, d_{yz} orbitals. Any increase in the negative ligand field along the z axis will destabilize d_{z^2} and decrease Δ. It is this effect that explains the much smaller Δ for Fe(TPP) in the solid than that found for the molecule in noncoordinating solvents. It could also explain the less than satisfactory temperature fit for Fe(PC) in which the close proximity of the rings in the solid could lead to a temperature dependence in Δ itself due to lattice changes with temperature.

In Fe(OEC) the negative value of δ indicates that the $^3B_3$ state is lower in energy, and this, in turn, means that the d_{xz} orbital is lower than the d_{yz} orbital in energy. This is consistent with what ligand field theory would predict. The presence of the pyrroline ring along the x axis should reduce the π interaction with d_{xz} but not that with d_{yz}. Since the electrons we are concerned with here are in antibonding orbitals, this results in the d_{yz} orbital being energetically higher. If π delocalization is dominated by the d_{yz} orbital only, we would expect a node along the x axis for the π orbital involved, and this appears to be borne out by the small value of ρ_π found for $-CH_2-$(g), which is close to the x axis. Thus the NMR data for Fe(OEC) is consistent with a ligand field model in which π bonding and spin delocalization through the d_{xz} orbital has been strongly reduced.

Although the theory seems adequate to explain the temperature dependence of the pseudocontact shift, it has trouble explaining some of the temperature dependences of the contact shift. The fits for all shifts in Fe(OEP) are good, as is the fit for the meso-H shifts in Fe(OEC). The problem occurs in explaining the pyrrole-H shift in Fe(TPP), the β-H shift in Fe(OEC), and the CH_2(g) shift in Fe(OEC). No adjustments of the parameters will explain these temperature effects. The values of ρ_π appear to be reasonable so there appears to be no need to question the assumption of π delocalization. We have tried introducing an anisotropy in the contact shift (which is known to be possible in systems with unquenched orbital momentum[27,28]) but this has not improved the situation measurably. Mispelter et al.[17] found some difficulty in fitting the temperature dependence of the contact shift with their theory and attributed it to neglecting excited quintet states in their calculations. The discrepancies found here are larger than they found, and a preliminary consideration of the effect of including the quintet states shows that we would obtain the same type of temperature functions. Thus the inclusion of quintet states would not remove the problem even if they were to make a sizable contribution to the shift. The only possible explanation that could be invoked is that Q and $(g_e\beta_e g_N\beta_N/R^3)$ are temperature dependent themselves. The β-H and CH_2 groups in Fe(OEC) have Q values that are known to be orientation dependent in similar free-radical systems, and we could be seeing here the effect of temperature averaging of different conformations with different values of Q. In the case of Fe(TPP), it is known that the molecule is strongly ruffled with the pyrroles having large displacements from the average plane of the molecule. In any case it appears that the pyrrole position is where the problem is most severe.

The NMR and susceptibility results clearly support a ground state of $^3A_{2g}$ for all the $S = 1$ iron(II) porphyrins studied here and a ^3E_gA ground state for Fe(PC) in the solid state. The results also agree with the electron density results.[13,14] The electron density results for Fe(TPP) were considered to be somewhere between the two states, but the analysis did not take into account

(27) McGarvey, B. R. In *Electronic Magnetic Resonance of the Solid State*; Weil, J., Ed.; The Chemical Institute of Canada: Ottawa, Ontario, Canada, 1987.
(28) McGarvey, B. R.; Nagy, S. *Inorg. Chem.* **1987**, *26*, 4198.

the spin–orbit interaction. I have found in the case of solid Fe(TPP) that $\Delta = 400$ cm^{-1}, and this means the $^3A_{2g}$ state is lowest before the spin–orbit interaction is taken into account. However after the spin–orbit interaction is included, the lowest state is only 74% $^3A_{2g}$ and the next state at 93 cm^{-1} is 73% $^3A_{2g}$. For Fe(PC) with $\Delta = -900$ cm^{-1} the lowest state is 100% ^3E_g, and the next states at 15 and 27 cm^{-1} are 13% and 23% $^3A_{2g}$, respectively.

Conclusion

It has been shown that the theory is adequate to explain the susceptibility and pseudocontact shift for four-coordinate ferrous porphyrin complexes of intermediate spin ($S = 1$) with symmetries less than axial in nature. The theory for the contact shift is less satisfactory, particularly for the β-pyrrole position when the macrocycle is ruffled in conformation.

Acknowledgment. This work was done while I was on sabbatical leave at Colorado State University, and I acknowledge the hospitality shown by the Department of Chemistry at CSU during my stay. I also acknowledge the help of Professor Strauss at CSU, who introduced me to the problem and helped with valuable discussions during the progress of the work. This work was supported in part by an operating grant from the Natural Sciences and Engineering Research Council of Canada.

Registry No. Fe(OEP), 61085-06-1; Fe(OEC), 78319-96-7; Fe(TPP), 16591-56-3; Fe(PC), 132-16-1.

Contribution from the Department of Chemistry and Center for Organometallic Research and Education, University of North Texas, Denton, Texas 76203, and Department of Medicinal Chemistry, College of Pharmacy, and Department of Chemistry, University of Houston, University Park, Houston, Texas 77004

Carbon-13 Relaxation and Reorientational Dynamics in a Bicapped Tetracobalt Cluster

M. Schwartz,[1a] M. G. Richmond,[1a,b] A. F. T. Chen,[1a] G. E. Martin,[1c] and J. K. Kochi*,[1d]

Received May 18, 1988

^{13}C spin–lattice (T_1) relaxation times and nuclear Overhauser enhancements of the phenyl (ortho, meta, and para) carbons in the tetracobalt cluster $Co_4(CO)_{10}(\mu_4\text{-}PPh)_2$ were measured as a function of temperature in $CDCl_3$. Three of the resonances exhibit triplet structure, indicating significant $^{31}P\cdots{}^{31}P$ interaction between the phosphinidene capping ligands. The rotational diffusion constants D_S ($=D_\parallel + R$) and $D_\perp$ derived from the T_1's reveal that the phenyl spinning rate (D_s) is approximately twice as rapid as molecular tumbling ($D_\perp$) at all temperatures. Comparison with the experimental diffusion constants in other systems suggests strongly that the phenyl rings do *not* undergo internal rotation ($R \approx 0$). This immobility is explained only partially by steric factors in the molecule. Comparison of the experimental results with diffusion constants calculated by the Perrin "stick" and Hu–Zwanzig "slip" models shows that the reorientational dynamics of the cluster is not well described by either of these limiting theories. Diffusion constants calculated by the newer Hynes–Kapral–Weinberg model provide the best agreement with the experimental results.

Introduction

The study of transition-metal clusters remains an active field due to their conceptual relationship to metal crystallites and heterogeneous catalysts, with newer interest stemming from the potential of polynuclear clusters to function as building blocks in the development of unusual electronic, magnetic, and optical materials.[2,3] Our previous studies have focused on the redox and ligand-substitution reactions of the tetracobalt cluster I whereas

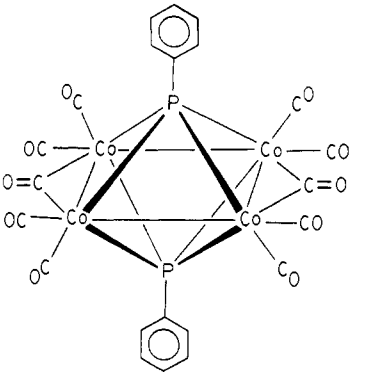

I

others have reported its catalytic activity.[4,5] While NMR investigations on I and various derivatives have been reported, no ^{13}C NMR data associated with the carbons of the phenylphosphinidene group have been reported. This dearth of data,

(1) (a) Department of Chemistry, University of North Texas. (b) Center for Organometallic Research and Education, University of North Texas. (c) Department of Medicinal Chemistry, College of Pharmacy, University of Houston. (d) Department of Chemistry, University of Houston.

(2) (a) Moskovits, M., Ed. *Metal Clusters*; Wiley-Interscience: New York, 1986; and references therein. (b) Gates, B. C.; Guczi, L.; Knozinger, H., Eds. *Metal Clusters in Catalysis*; Elsevier: New York, 1986; and references therein. (c) Lewis, J.; Green, M. L. H., Eds. *Metal Clusters in Chemistry*; Cambridge University Press: Cambridge, England, 1982; and references therein. (d) Johnson, B. F. G., Ed. *Transition Metal Clusters*; Wiley: New York, 1980; and references therein.

(3) (a) Vahrenkamp, H. *Adv. Organomet. Chem.* **1983**, *22*, 169. (b) Muetterties, E. L. *Science (Washington, D.C.)* **1977**, *196*, 839. (c) Muetterties, E. L.; Rhodin, T. N.; Band, E.; Brucker, C. F.; Pretzer, W. R. *Chem. Rev.* **1979**, *79*, 91. (d) Muetterties, E. L. *J. Organomet. Chem.* **1980**, *200*, 177. (e) Muetterties, E. L.; Krause, M. J. *Angew. Chem., Int. Ed. Engl.* **1983**, *22*, 135. (f) Smith, A. K.; Basset, J. M. *J. Mol. Catal.* **1977**, *2*, 229. (g) Gladfelter, W. L. *Adv. Organomet. Chem.* **1985**, *24*, 41. (h) Adams, R. D. *Acc. Chem. Res.* **1983**, *16*, 67. (i) Adams, R. D.; Horvath, I. T. *Prog. Inorg. Chem.* **1985**, *32*, 127.

(4) (a) Richmond, M. G.; Kochi, J. K. *Inorg. Chem.* **1986**, *25*, 656, 1334. (b) Richmond, M. G.; Kochi, J. K. *Organometallics* **1987**, *6*, 254.

(5) (a) Pittman, C. U.; Wilemon, G. M.; Wilson, W. D.; Ryan, R. C. *Angew. Chem., Int. Ed. Engl.* **1980**, *19*, 478. (b) Ryan, R. C.; Pittman, C. U.; O'Connor, J. P. *J. Am. Chem. Soc.* **1977**, *99*, 1980. (c) Pittman, C. U.; Richmond, M. G.; Wilemon, G. M.; Absi-Halabi, M. In *Catalysis of Organic Reactions*; Kosak, J. R., Ed.; Dekker: New York, 1984; Chapter 5. (d) Wang, Y. P.; Zhang, S. M.; Wu, N.; Luo, Y. Z.; Fu, H. X. *J. Organomet. Chem.* **1986**, *307*, 65.

0020-1669/88/1327-4698$01.50/0 © 1988 American Chemical Society